

Study on the Preparation and Tribological Properties of Fly Ash as Lubricant Additive for Steel/Steel Pair

Zhengfeng Cao¹ · Yanqiu Xia¹

Received: 27 March 2017 / Accepted: 21 June 2017 / Published online: 3 July 2017
© Springer Science+Business Media, LLC 2017

Abstract Fly ash, generated during the combustion of coal for energy production, has been regarded as an environmental pollutant if not properly disposed of. Many aggressive efforts have been evaluated to recycle the fly ash. In this paper, a new approach was developed to prepare lubricant additive based on fly ash and the tribological properties were investigated in detail. The results show that fly ash modified with oleic acid not only performs favorable dispersive ability, but also significantly improves the friction-reducing and anti-wear abilities for steel/steel contact. Based on the characterization of the wear scars by scanning electron microscopy, Raman spectroscopy and energy-dispersive X-ray spectroscopy, the excellent tribological properties are attributed to the synergies of fly ash and oleic acid because fly ash can act as spacer and bearing and deposit on the worn surfaces to significantly improve the friction-reducing and anti-wear abilities, and the introduction of strong polar groups can make fly ash easily form a stable and successive tribofilm on the rubbing surfaces throughout the sliding process.

Keywords Fly ash · Oleic acid · Lubricant additive · Tribology

1 Introduction

Friction which is an essential characteristic of contacts in motion leads to the failure of most mechanical parts and consumption in energy [1]. It cannot be eliminated, but can be controlled by employing lubricants to improve the tribological performances. Given the world's energy crisis, there have been increasing demands for environmental protection and the reliability assurance of mechanical equipment, so it is particularly imperative to develop green, inexpensive, effective and versatile lubricant additives [2–4]. Ionic liquids, graphene and carbon nanotubes have been explored as excellent lubricant additives for a long time, whereas there are still some problems such as corrosion, dispersion and cost, which limit actual application in industry [5–7]. Thus, a continuous desire also exists to explore new lubricant additives.

Fly ash, a by-product of thermal power plants, is recognized as an environmental pollutant if not properly disposed of [8, 9]. It is primarily composed of unburned carbon and oxides of silicon, aluminum, iron, etc. The density and grain size of fly ash as received from the power plants lie in the range from 0.1 to 250 μm and 1.9 to 2.9 g cm^{-3} , respectively [10–12]. Fly ash also has a high porosity and a large special surface area, indicating a strong adsorption ability [13, 14]. Due to the world's increasing dependence on coal-fired power plants, the current annual production of fly ash worldwide is estimated around 750 million tones [15]. Fly ash without proper dispose can cause water and soil pollution, disrupt ecological cycles and pose environment hazards; therefore, more aggressive efforts have been attempted to recycle fly ash [16–18]. For example, it has been widely used in concrete production [19, 20], ceramic industry [21], soil amendment [22, 23], zeolite synthesis [24, 25] and

✉ Yanqiu Xia
xiayq@ncepu.edu.cn

¹ School of Energy Power and Mechanical Engineering, North China Electric Power University, Beijing 102206, China

Table 1 Typical characteristics of polyalphaolefin (PAO)

Item	PAO	Standard
Kinematic viscosity(cSt) 40 °C	396	ASTM D445
Kinematic viscosity(cSt) 100 °C	39	ASTM D445
Viscosity index	147	ASTM D2270
Pour point (°C)	−36	ASTM D97
Fire point (°C)	281	ASTM D2893

polymers [26]. In addition, fly ash has been also widely used in the field of lubrication. Sudarshan et al. [27] fabricated alloy composites containing fly ash via stir-cast technique. The results showed that alloy composites exhibited better anti-wear performance compared to unreinforced alloy, which was attributed to the rolling effect of fly ash during the sliding process. Samrat et al. [28] incorporated fly ash particles in automotive brake lining friction composites and found the developed composites exhibited stable coefficient of friction and low wear rate. Harekrushna et al. [29] obtained fly ash added red mud coatings by plasma spraying technique and investigated the tribological performances. The results showed that the addition of fly ash greatly improved the anti-wear property. A number of studies have been successfully made to introduce fly ash to improve the tribological properties, whereas fly ash used as an additive in lubricant, to the best of our knowledge, has not been reported.

The related studies [30–32] have reported that micro/nano-particles can significantly enhance the tribological properties; therefore, it is possible to explore fly ash as a lubricant additive to improve tribological properties. If the fly ash could be as effective as expected, it provides a new approach to obtain low-cost lubricant additive and recycle it. Therefore, the focus of present work is to prepare lubricant additive based on fly ash and investigate the tribological properties in detail. In the meanwhile, because the dispersive ability of solid additive has a significant effect on the tribological properties, therefore, the oleic acid is introduced as surfactant to modify the fly ash to improve the dispersive

and tribological performances. Furthermore, the present study also discusses the tribological mechanisms via scanning electron microscopy (SEM), energy-dispersive X-ray spectroscopy (EDS) and Raman spectroscopy.

2 Experimental Detail

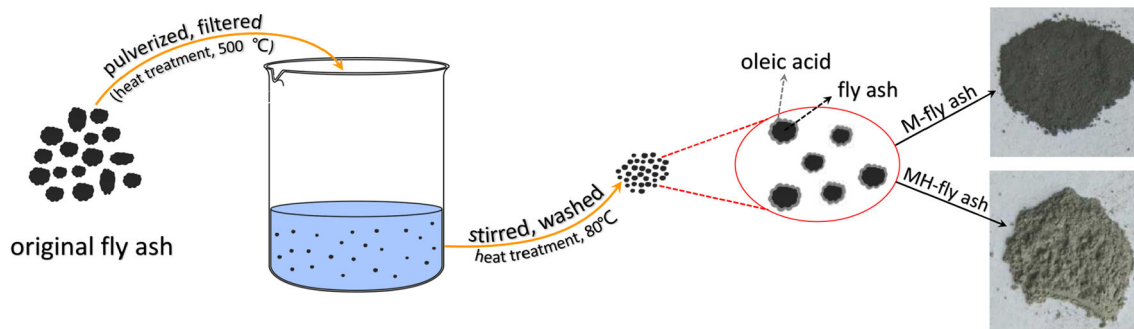
2.1 Materials

The polyalphaolefin (PAO) used as the base oil was purchased from Golden Chemical Co. Ltd. (Nanjing, China), and Table 1 shows its main characteristics. Acetone, petroleum ether and oleic acid were purchased from Sino-pharm Chemical Reagent Co. Ltd, and they are of analytical reagent grade. Polytetrafluoroethylene (PTFE, Dyneon™ TF9207), with a density of 2.2 g cm^{-3} and $4 \mu\text{m}$ grain size, was used as a thickener to thicken the base oil for lubricating grease. The fly ash without purification was provided by the Jungar Power Plant (Inner Mongolia, China), and the composition of the fly ash is (mass fraction): SiO_2 41.3%, Al_2O_3 27.6%, Fe_2O_3 8.3%, TiO_2 4.5%, MgO 1.8%, unburned carbon 12.7% and other 3.8%.

2.2 Preparation and Characterization

2.2.1 Preparation of Lubricant Additives

The target lubricating additives were synthesized as the following procedures, and Fig. 1 is the schematic diagram of preparation. First, a part of fly ash was heat-treated using a muffle furnace at 500 °C for 12 h. Second, the cooling product (denoted as H-fly ash) and untreated fly ash (denoted as fly ash) were pulverized using a ball mill, respectively. The experimental parameters of ball milling are as follows: The weight ratio of fly ash and grinding ball is about 1/10, and the rotational speed of ball mill is $\sim 900 \text{ r min}^{-1}$ for 5 h. Third, the pulverized fly ash was filtered and then introduced into the vessel for 12 h of a fierce agitation in bath of oleic acid whose mass was about

**Fig. 1** Schematic diagram of preparation of lubricant additives

three times of fly ash. Finally, the mixtures were washed with acetone several times followed by a desiccation for 30 min at 80 °C. Thus, four types of lubricating additives (fly ash, modified fly ash, treated fly ash and modified treated fly ash) were obtained and they were abbreviated as fly ash, M-fly ash, H-fly ash and MH-fly ash, respectively.

2.2.2 Preparation of Lubricating Oils and Lubricating Greases

The lubricating oils and lubricating greases were synthesized as follows. The obtained additives (content 0.2 wt%) were added into PAO severally and were evenly dispersed by ultrasonic processing for 30 min to afford lubricating oils.

The as-synthesized lubricating oils were used as the base oils to prepare lubricating greases. First, the base oil (70 wt%) was infused into the reaction vessel and agitated at once. Second, the PTFE as a thickener (30 wt%) was slowly added into the vessel under vigorous stirring. As the base oil was blended homogeneously with the PTFE powder, acetone, whose mass was approximately half of the PTFE, was injected dropwise and agitated for about 30 min to confirm that PTFE powder was entirely homo-dispersed within the base oil. Third, the mixture was heated to 80 °C for another 30 min to remove acetone. Last, the mixture was cooled down to room temperature and the lubricating greases were obtained after three steps of fine grinding/homogenization with a three-roller mill.

2.2.3 Characterization of the Additives and Lubricating Greases

The morphology of the pulverized fly ash was obtained by a SU8010 scanning electron microscopy (SEM) (HITACHI, Japan). The Fourier transform infrared (FT-IR) spectra of lubricating additives were recorded in the wavenumber range of 400–4000 cm^{-1} with a Thermo Fisher Scientific FT-IR spectrometer. Their Raman spectra were obtained by Renishaw in via Raman microscopy with 514 nm laser excitation. The penetration, dropping point and copper strip tests of the lubricants were determined according to the national standards, including GB/T 269, GB/T 3498 and GB/T 7326, respectively.

2.3 Friction and Wear Tests

The tribological properties of the lubricants for steel/steel contact were investigated on a ball-on-block **MFT-R4000 reciprocating friction and wear tester**. The upper ball (commercially available AISI 52100 steel ball, diameter 5 mm, hardness 710 Hv, surface roughness 0.05 μm) was driven to reciprocally slide at an amplitude of 5 mm

against the lower fixed block (Φ 24 mm \times 7.9 mm, AISI 52100 steel, hardness 590–610 Hv). The lower blocks were polished using a polishing machine to achieve the surface roughness of about 0.05 μm before test. The applied load ranges from 50 to 200 N (corresponding to the Hertzian pressure in the range of 1.7–2.7 GPa) with the frequency of 5 Hz for 30 min at room temperature (RT). Before every tribological test, the ball and block were cleansed in petroleum ether for 10 min utilizing an ultrasonic cleaner and then about 0.5 g of lubricant was introduced into the reciprocating sliding region. The coefficient of friction (COF) was automatically recorded by a computer connected with the tribometer, and three repetitive measurements were taken to guarantee the reliability of the experimental data. After the tribological test, the lower blocks were cleaned ultrasonically for 10 min in bath of petroleum ether. Then, an optical microscopy (Olympus, Japan) was employed to acquire the wear width. An EVO-18 scanning electron microscopy (SEM, Zeiss, Germany), an energy-dispersive X-ray spectroscopy (EDS, Bruker, Germany) and a Raman spectroscopy with 514 nm laser excitation (Renishaw, UK) were employed to obtain the morphologies of the worn surfaces and analyze the wear mechanisms.

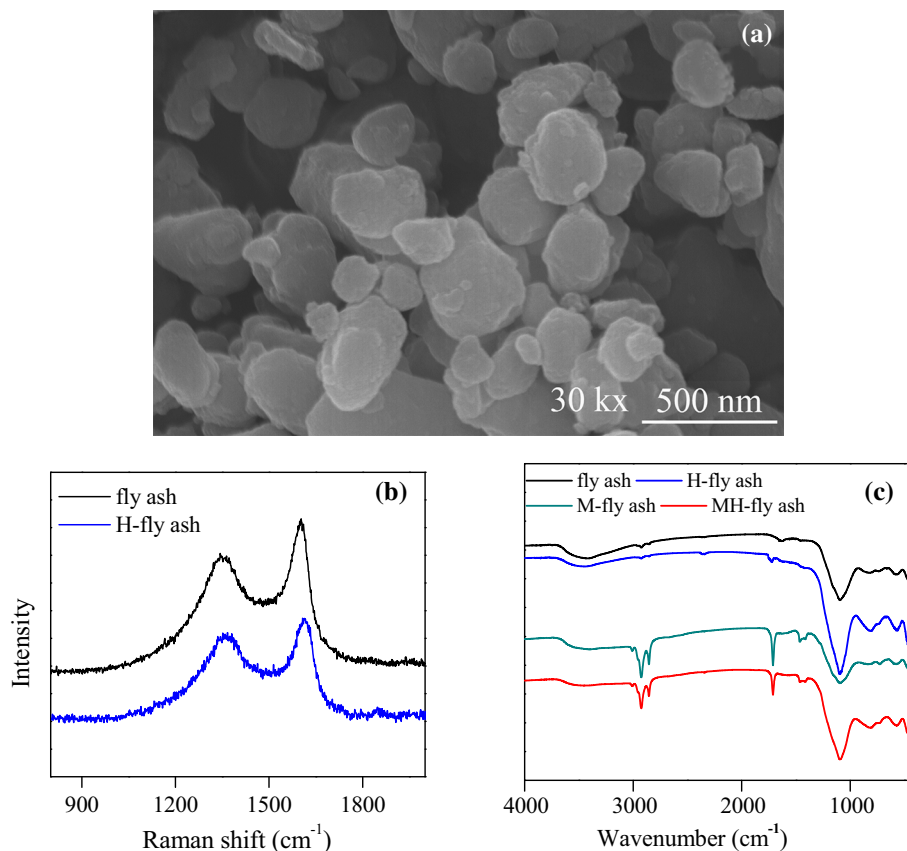
3 Results

3.1 Analysis of the Additives

Figure 2a shows the SEM micrograph of the filtered fly ash. It is obviously seen that the fly ash has multiple shapes and uneven sizes, which range from about 150 to 600 nm. The Raman spectra of fly ash and H-fly ash are shown in Fig. 2b. The fly ash shows the characteristic peaks of D band (\sim 1340 cm^{-1}) and G band (\sim 1600 cm^{-1}), which originate from the vibration of carbon atoms with dangling bonds and vibration in all sp^2 -bonded carbon atoms, respectively [33], thereby indicating that fly ash contains a large amount of unburned carbon. Obratsova et al. [34] reported that shell curvature caused a downshift of G band position in spherical carbon compared with that in planar graphite (1580 cm^{-1}). As a consequence, the position of G band is determined by outmost shell in the Raman spectra, which explains the G band shifts to a high frequency due to the larger size and defects of unburned carbon [35, 36].

The FT-IR spectra of lubricant additives are presented in Fig. 2c. The wide band at about 3525 cm^{-1} is attributed to the stretching vibration of O–H [36], and those bands at 1080 and 798 cm^{-1} are attributed to the stretching vibrations of Si–O–Si and Al–O–Al [37, 38]. The band at 570 cm^{-1} (stretching vibration of Al–O–Al) and 466 cm^{-1} (bending vibration of Si–O–Si and O–Si–O) is also

Fig. 2 SEM micrograph (a), Raman spectra (b) and FT-IR spectra (c) of lubricating additives



indicative of silicate [37]. H-fly ash was observed to have a strong band at 1720 cm^{-1} which indicated the presence of C=O originates from the oxide of annealed fly ash. The bands of oleic acid are located at 2930 and 2850 cm^{-1} (stretching vibrations of C–H bond in the $-\text{CH}_3$ and $-\text{CH}_2$ groups) and 1705 and 1455 cm^{-1} (stretching vibration of C = O and $-\text{COOH}$) [36].

Figure 3 presents the photograph of the PAO with addition of four types of lubricant additives after storage for 168 h. It can be confirmed that the M-fly ash and MH-

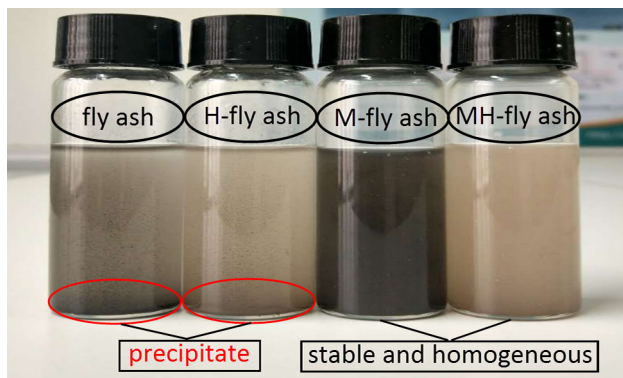


Fig. 3 Photograph of PAO with addition of four types of lubricant additives after storage for 168 h

fly ash perform better dispersion and stability, indicating the tentative modification of fly ash with oleic acid is successful. Of great significance is that the M-fly ash and MH-fly ash with good dispersion can effectively adsorb on the sliding surfaces to form a low-shear protective film to improve the tribological properties.

3.2 Physical Properties of Lubricating Greases

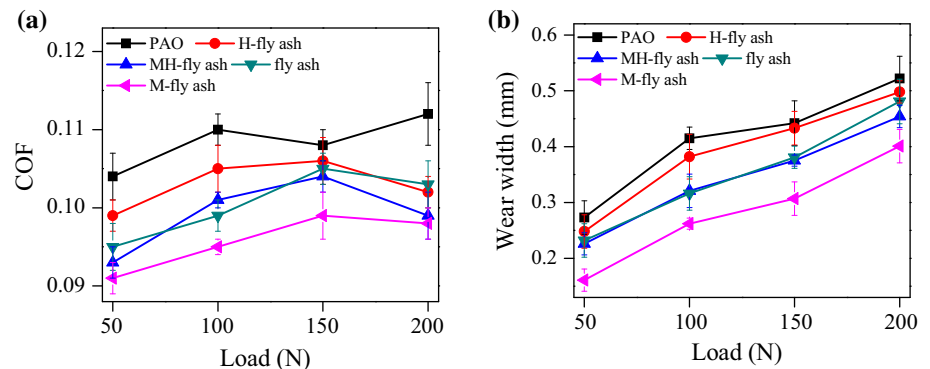
Table 2 lists the physical properties of the additive-contained greases. Compared with base grease, all the additive-doped greases have high dropping point and low penetration. The reason is ascribed that the as-synthesized additives with a high special surface area can restrict the movement of base oil molecules, then leading to a high dropping point and a low penetration [39, 40]. Meanwhile, all the lubricating greases exhibit a good anti-corrosion performance (copper corrosion 1a).

3.3 Tribological Behavior of Lubricating Oils

Figure 4 presents mean COFs and wear widths of the lubricating oils, which contain 0.2 wt% additive, at multiple loads, 5 Hz and RT. The results illustrate that all the additives have a preferable effect on the friction-reducing

Table 2 Physical properties of lubricating greases

Sample	Dropping point (°C)	Penetration (1/4 mm)	Copper corrosion (T2 copper, 100 °C, 24 h)
Base grease	279	87.3	1a
Fly ash grease	296	82.1	1a
M-fly ash grease	294	81.9	1a
H-fly ash grease	291	82.4	1a
MH-fly ash grease	297	83.1	1a

Fig. 4 Evolution of average COFs (a) and average wear widths (b) for the lubricating oils at different loads, 5 Hz and RT

and anti-wear properties. The COFs and wear widths of the MH-fly ash and M-fly ash are lower than those of H-fly ash and fly ash at different loads, respectively. The most significant improvement for lubricity is obtained by the PAO with the addition of M-fly ash, reducing the COF and wear width by ~ 14 and $\sim 37\%$. This demonstrates that the PAO with the adding amount of M-fly ash possesses the most excellent friction reduction and anti-wear performances than other lubricating oils.

Figure 5 provides the morphologies of the worn surfaces on steel blocks at 200 N, 5 Hz, and all the SEM morphologies are obtained at the same condition. As shown in Fig. 5a and a', the worn surfaces lubricated by PAO display a considerably wider and deeper wear scar, with a plenty of deep furrows and large pits, indicating severe wear occurred on this occasion. The addition of H-fly ash and fly ash can make the worn surfaces (Fig. 5b-b', d-d') slightly become smooth, with little pits and slight plastic deformation. The worn surfaces (Fig. 5c-c', e-e') lubricated by MH-fly ash and M-fly ash appear smaller and smoother wear scars. This is consistent with the previous results in Fig. 4, illustrating MH-fly ash and M-fly ash as additives in PAO can significantly improve the friction reduction and anti-wear performances.

3.4 Tribological Behavior of Lubricating Greases

The experimental results shown in Fig. 4 and 5 reveal that MH-fly ash and H-fly ash have an effective improvement

on tribological performances. Therefore, this study continues to investigate the effect of MH-fly ash and M-fly ash on the tribological properties of lubricating greases. Figure 6 shows the mean COFs and wear widths of the lubricating greases at different loads, 5 Hz and RT. It is seen that the mean COFs and wear widths of all additive-contained greases are lower than those of base grease and increase as the load growing, to some extent. The M-fly ash grease exhibits the lowest COF and wear width at different loads, implying the best friction reduction and anti-wear abilities among the greases.

Figure 7 displays the SEM graphologies of worn surfaces on steel blocks at 200 N and 5 Hz. As shown in Fig. 7a and a', the worn surface lubricated by base grease acquires a wide wear scar and deep grinding grooves, whereas the worn surfaces (Fig. 7b-b', c-c') lubricated by MH-fly ash grease and M-fly ash grease are relatively smooth, which is attributed to the significant improvement of MH-fly ash and M-fly ash on the tribological properties for lubricating grease.

3.5 Lubrication Mechanisms

The worn surfaces on steel blocks after ultrasonic washing were further checked with EDS and Raman spectroscopy to explore the tribological mechanisms. Figure 8 provides the Raman spectra of the worn surfaces lubricated by M-fly ash grease and MH-fly ash grease. For the M-fly ash and MH-fly ash tested in our study, the

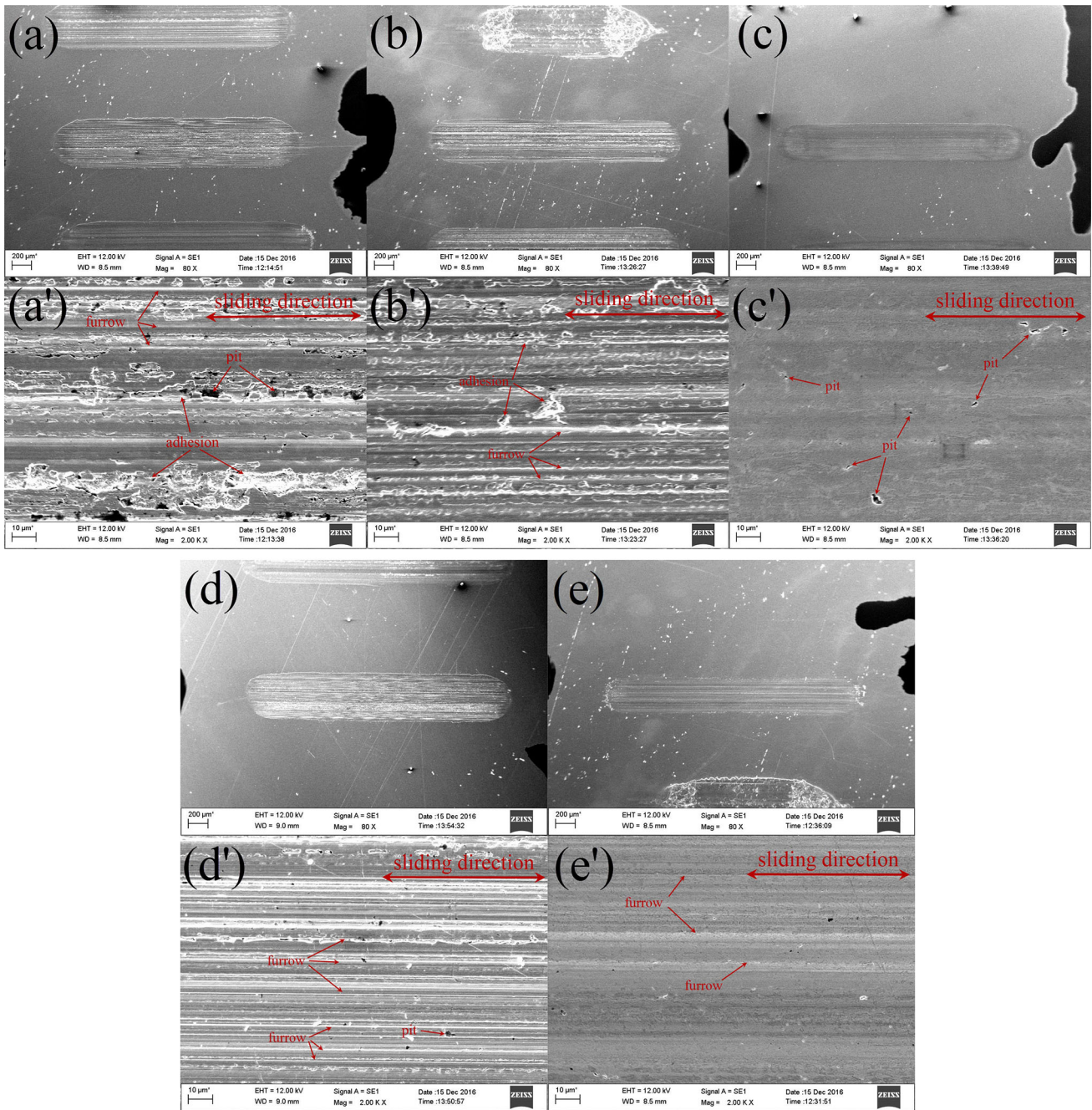


Fig. 5 SEM morphologies of the worn surfaces lubricated by **a** and **a'** PAO, **b** and **b'** H-fly ash oil, **c** and **c'** MH-fly ash oil, **d** and **d'** fly ash oil, **e** and **e'** M-fly ash oil. (magnification: *top* images, $\times 80$; and

bottom images, $\times 2000$; load, 200 N; frequency, 5 Hz; stroke, 5 mm; duration, 30 min; temperature, RT)

characteristics G and D bands can be clearly observed on worn surfaces after friction test, indicating a carbon protective film was formed on the worn surfaces during the sliding process. Table 3 lists the typical elements and their contents on the worn surfaces lubricated by different lubricants. The characteristics Al and Si elements of the fly ash appear on the worn surfaces, implying fly ash deposited on the worn surfaces to form protective film

throughout frictional process. Meanwhile, the content of C element on the worn surfaces lubricated by M-fly ash oil and M-fly ash grease is the largest. Those elements have a crucial influence on the friction reduction and anti-wear performances. It is presumed that an effectively protective film is formed on the worn surfaces by complex physical and chemical reaction to improve the tribological properties.

Fig. 6 Evolution of average COFs (a) and average wear widths (b) for the lubricating greases at different loads, 5 Hz and RT

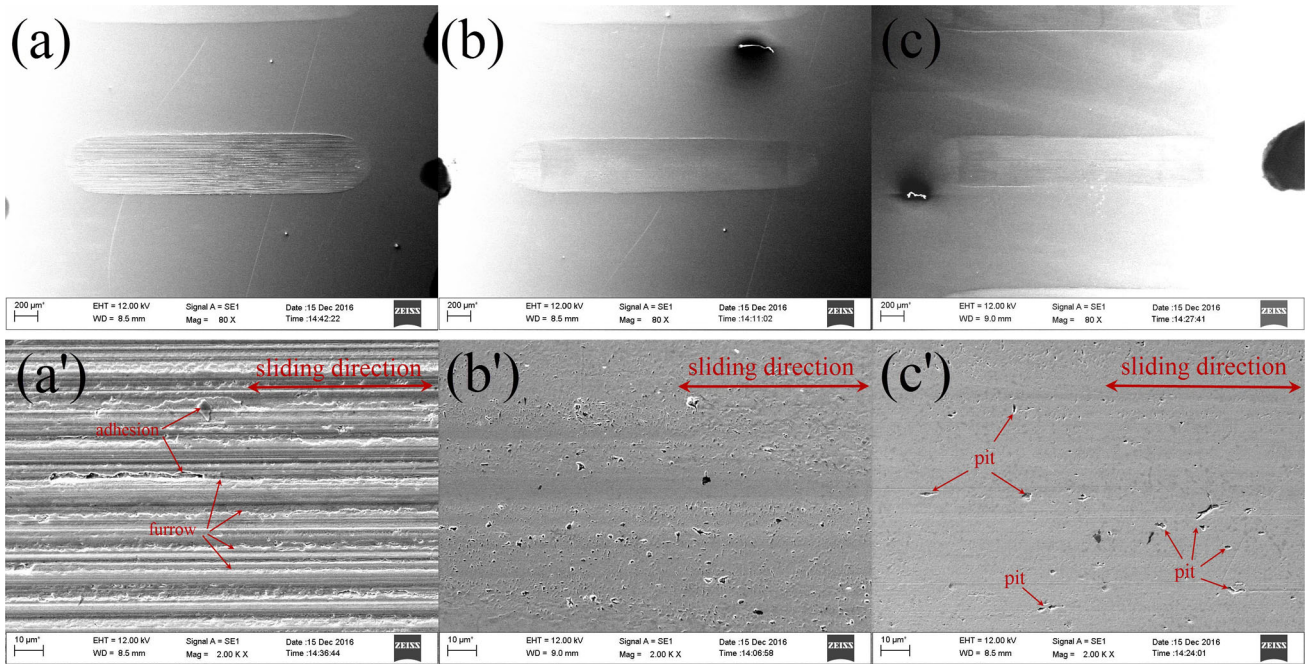
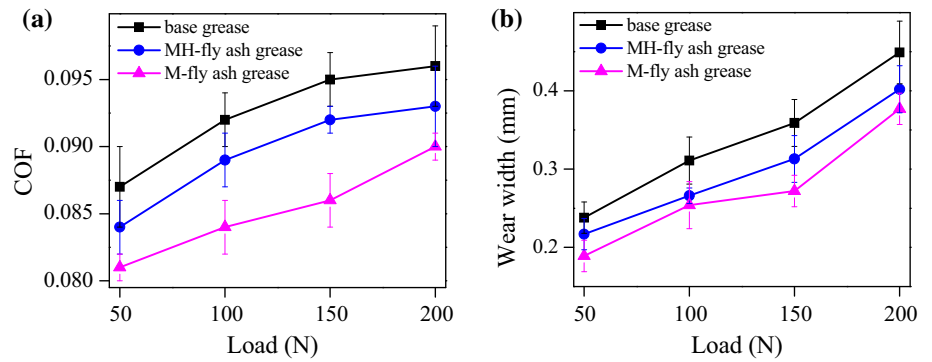


Fig. 7 SEM morphologies of the worn surfaces lubricated by a and a' base grease, b and b' MH-fly ash grease, c and c' M-fly ash grease. (magnification: top images, $\times 80$; and bottom images, $\times 2000$; load, 200 N; frequency, 5 Hz; stroke, 5 mm; duration, 30 min; temperature, RT)

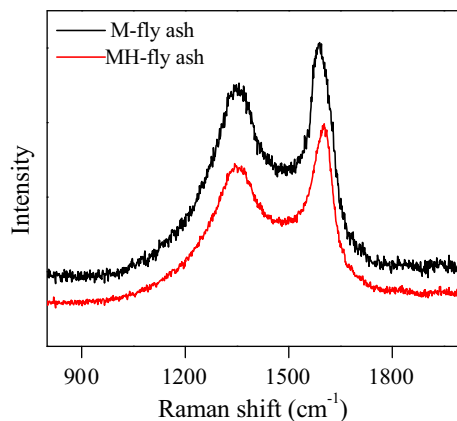


Fig. 8 Raman spectra of the worn surfaces lubricated by M-fly ash grease and MH-fly ash grease

Table 3 Typical elements of the worn surfaces on the steel blocks

Sample	Fe	Cr	C	O	Al	Si
Base oil (PAO)	83.10	1.97	6.86	8.07	–	–
H-fly ash	81.86	1.62	8.03	7.91	0.26	0.32
MH-fly ash	82.59	1.95	7.28	7.53	0.24	0.41
Fly ash	80.85	1.45	8.78	8.21	0.36	0.35
M-fly ash	80.10	1.78	9.61	7.85	0.29	0.37
Base grease	86.01	1.70	6.28	6.01	–	–
MH-fly ash	83.29	1.80	7.84	6.53	0.23	0.31
M-fly ash	82.75	1.78	8.83	5.98	0.26	0.40

The tribological tests and analysis of the morphological features of the worn surfaces show that fly ash as additive can significantly improve the friction reduction and anti-wear abilities for lubricating oil and grease. This result inspires us to further explore the conceivable lubrication mechanisms of fly ash. Based on the characterization by SEM, Raman spectra and EDS, the enhancement in tribological properties of fly ash can be explained by various aspects. First, the lubricants can uniformly settle down between the contact surfaces. Fly ash can fill in the valley of surfaces to increase contact area and perform like spacers to avoid direct contact between the contact interfaces during the course of friction [41, 42]. Second, the spherical fly ash also has rolling effect, which implies fly ash would roll instead of slide between the contact interfaces, thereby reducing the shear force to improve the tribological properties [27, 43–46]. Third, the appearance of Al and Si on the worn surfaces (shown in Table 3) illustrates that the fly ash would deposit on the worn surfaces to enhance the protective film during the sliding process. Furthermore, Raman spectra with a downshift of G band (1590 cm^{-1} , shown in Fig. 8) also indicates that layered carbon is generated during the sliding process, and it can also slide between the contact pair to improve the tribological properties. This phenomenon is similar to the onion-like carbon under friction condition, and the mechanism is also reported by Wei et al. and Bucholz et al. [36, 47]. As for the M-fly ash and MH-fly ash, the introduction of strong polar groups can greatly improve the dispersive ability, which indicates the M-fly ash and MH-fly ash can more easily adsorb on the worn surfaces to form a stable and successive lubrication film throughout the sliding process. Meanwhile, the related studies [48, 49] reveal that oleic acid can also form lubrication film on the worn surfaces to improve the friction-reducing and anti-wear abilities. Consequently, the synergies of fly ash and oleic acid give rise to the enhancement in the friction reduction and anti-wear abilities of lubricants.

4 Conclusions

Fly ash as a solid waste causes a lot of environmental pollution every year, and intensive efforts have been made to recycle it. In this study, lubricant additives were prepared based on fly ash and oleic acid was introduced to improve the dispersive ability. Results show that fly ash modified with oleic acid as an additive has an excellent dispersibility and tribological properties. The reason lies in the synergies of fly ash and oleic acid, because fly ash can act as spacer and bearing and deposit on the worn surfaces to significantly improve the friction reduction and anti-wear abilities, and the introduction of strong polar groups

can make fly ash easily form a stable and successive tribofilm on the rubbing surfaces throughout the sliding process. This paper provides a new approach to obtain low-cost lubricant additive and dispose of fly ash properly to reduce environmental pollution. Because of the excellent tribological performances, fly ash holds great potential as a solid lubricant for a wide range of application.

Acknowledgements This work is supported by the National Natural Science Foundation of China (Grant 51575181) and Beijing Natural Science Foundation (Grant 2172053).

References

- Matta, C., Jolyptottuz, L., Bouchet, M.D.B., Martin, J.M., Kano, M., Zhang, Q., Goddard, W.A.: Superlubricity and tribochemistry of polyhydric alcohols. *Phys. Rev. B: Condens. Matter Mater. Phys.* **78**, 1–8 (2008)
- Boyde, S.: Green lubricants: environmental benefits and impacts on lubrication. *Green Chem.* **4**, 293–307 (2002)
- Xia, Y.Q., Xu, X.C., Feng, X., Chen, G.X.: Leaf-surface wax of desert plants as a potential lubricant additive. *Friction* **3**, 208–213 (2015)
- Shi, Y.J., Minami, I., Grahm, M., Bjorling, M., Larsson, R.: Boundary and elastohydrodynamic lubrication studies of glycerol aqueous solutions as green lubricants. *Tribol. Int.* **69**, 39–45 (2014)
- Liu, X., Zhou, F., Liang, Y., Liu, W.: Benzotriazole as the additive for ionic liquid lubricant: one pathway towards actual application of ionic liquids. *Tribol. Lett.* **23**, 191–196 (2006)
- Rastogi, R., Kaushal, R., Tripathi, S.K., Sharma, A.L., Kaur, I., Bharadwaj, L.M.: Comparative study of carbon nanotube dispersion using surfactants. *J. Colloid Interface Sci.* **328**, 421–428 (2008)
- Cai, M., Liang, Y., Zhou, F., Liu, W.: Tribological properties of novel imidazolium ionic liquids bearing benzotriazole group as the antiwear/anticorrosion additive in poly (ethylene glycol) and polyurea grease for steel/steel contacts. *ACS Appl. Mater. Interfaces* **3**, 4580–4592 (2011)
- Ahmaruzzaman, M.: A review on the utilization of fly ash. *Prog. Energy Combust. Sci.* **36**, 327–363 (2010)
- Wee, J.H.: A review on carbon dioxide capture and storage technology using coal fly ash. *Appl. Energy* **106**, 143–151 (2013)
- Altun, N.E., Xiao, C., Hwang, J.Y.: Separation of unburned carbon from fly ash using a concurrent flotation column. *Fuel Process. Technol.* **90**, 1464–1470 (2009)
- Rohatgi, P.K., Guo, R.Q.: Mechanism of abrasive wear of Al–Si hypoeutectic alloy containing 5 vol% fly ash. *Tribol. Lett.* **3**, 339–347 (1997)
- Hintsho, N., Shaikjee, A., Masenda, H., Naidoo, D., Billing, D., Franklyn, P.: Direct synthesis of carbon nanofibers from South African coal fly ash. *Nanoscale Res. Lett.* **9**, 387 (2014)
- Zhang, Y., Duan, W., Liu, Z., Cao, Y.: Effects of modified fly ash on mercury adsorption ability in an entrained-flow reactor. *Fuel* **128**, 274–280 (2014)
- Hunter, T., Alexander, C.B., Cooper, J.A.: Adsorption of an acid dye onto coal fly ash. *Fuel* **87**, 3040–3045 (2008)
- Blissett, R.S., Rowson, N.A.: A review of the multi-component utilisation of coal fly ash. *Fuel* **97**, 1–23 (2012)
- Yao, Z.T., Ji, X.S., Sarker, P.K., Tang, J.H., Ge, L.Q., Xia, M.S.: A comprehensive review on the applications of coal fly ash. *Earth-Sci. Rev.* **141**, 105–121 (2015)

17. Yao, Z.T., Xia, M.S., Sarker, P.K., Chen, T.: A review of the alumina recovery from coal fly ash, with a focus in China. *Fuel* **120**, 74–85 (2014)
18. Manoharan, V., Yunusa, I.A.M., Loganathan, P., Lawrie, R., Skilbeck, C.G., Burchett, M.D.: Assessments of class F fly ashes for amelioration of soil acidity and their influence on growth and uptake of Mo and Se by canola. *Fuel* **89**, 3498–3504 (2010)
19. Sumajouw, D.M.J., Wallah, S.E., Hardjito, D.: On the development of fly ash-based geopolymer concrete. *ACI Mater. J.* **101**, 467–472 (2004)
20. Bouzoubaâ, N., Lachemi, M.: Self-compacting concrete incorporating high volumes of class F fly ash: preliminary results. *Cem. Concr. Res.* **31**, 413–420 (2001)
21. Yao, Z., Tan, S., Xia, M., Ye, Y., Li, J.: Synthesis, characterization and sintering behaviour of indialite ceramic from fly ash. *Waste Manag. Res.* **29**, 1090–1097 (2011)
22. Lee, H., Ha, H.S., Lee, C.H., Lee, Y.B., Kim, P.J.: Fly ash effect on improving soil properties and rice productivity in Korean paddy soils. *Bioresour. Technol.* **97**, 1490–1497 (2006)
23. Matsi, T., Keramidias, V.Z.: Fly ash application on two acid soils and its effect on soil salinity, pH, B, P and on ryegrass growth and composition. *Environ. Pollut.* **104**, 107–112 (1999)
24. Querol, X., Moreno, N., Umaña, J.C., Alastuey, A., Hernández, E., López-Soler, A.: Synthesis of zeolites from coal fly ash: an overview. *Int. J. Coal Geol.* **50**, 413–423 (2002)
25. Yao, Z., Ye, Y., Xia, M.: Synthesis and characterization of lithium zeolites with ABW type from coal fly ash. *Environ. Prog. Sustain. Energy* **32**, 790–796 (2013)
26. Ramakrishna, H.V., Priya, S.P., Rai, S.K.: Utilization of flyash as filler for polybutyleneterephthalate-toughened epoxy resin. *Polym. Eng. Sci.* **46**, 946–953 (2006)
27. Sudarshan, Surappa, M.K.: Dry sliding wear of fly ash particle reinforced A356 Al composites. *Wear* **265**, 349–360 (2008)
28. Mohanty, S., Chugh, Y.P.: Development of fly ash-based automotive brake lining. *Tribol. Int.* **40**, 1217–1224 (2007)
29. Sutar, H., Roy, D., Mishra, S.C., Chakraverty, A.P., Maharana, H.S.: Friction and wear behaviour of plasma sprayed fly ash added red mud coatings. *Phys. Sci. Int. J.* **5**, 61–73 (2014)
30. Schwarz, U.D., Zwörner, O., Köster, P., Wiesendanger, R.: Quantitative analysis of the frictional properties of solid materials at low loads. I. Carbon compounds. *Phys. Rev. B* **56**, 6987–6996 (1997)
31. Peng, D., Chen, C., Kang, Y., Chang, Y., Chang, S.: Size effects of SiO₂ nanoparticles as oil additives on tribology of lubricant. *Ind. Lubr. Tribol.* **62**, 111–120 (2010)
32. Sun, X.F., Qiao, Y.L., He, J.W., Ma, S.N., Hu, C.H.: High temperature tribological behavior of nano-Al₂O₃ in different base oils. *Key Eng. Mater.* **373–374**, 568–571 (2008)
33. He, C., Zhao, N., Shi, C., Du, X., Li, J., Cui, L.: A practical method for the production of hollow carbon onion particles. *J. Alloys Compd.* **425**, 329–333 (2006)
34. Obratsova, E.D., Fujii, M., Hayashi, S., Kuznetsov, V.L., Butenko, Y.V., Chuvilin, A.L.: Raman identification of onion-like carbon. *Carbon* **36**, 821–826 (1998)
35. Choucair, M., Stride, J.A.: The gram-scale synthesis of carbon onions. *Carbon* **50**, 1109–1115 (2012)
36. Wei, J., Cai, M., Feng, Z., Liu, W.: Candle soot as particular lubricant additives. *Tribol. Lett.* **53**, 521–531 (2014)
37. Lee, W.K.W., Deventer, J.S.J.V.: Structural reorganisation of class F fly ash in alkaline silicate solutions. *Colloids Surf. A* **211**, 49–66 (2002)
38. Vempati, R.K., Rao, A., Hess, T.R., Cocke, D.L., Lauer Jr., H.V.: Fractionation and characterization of Texas lignite class 'F' fly ash by XRD, TGA, FTIR, and SFM. *Cem. Concr. Res.* **24**, 1153–1164 (1994)
39. Cao, Z., Xia, Y., Ge, X.: Conductive capacity and tribological properties of several carbon materials in conductive greases. *Ind. Lubr. Tribol.* **68**, 577–585 (2016)
40. Ge, X.Y., Xia, Y.Q., Feng, X.: Influence of carbon nanotubes on conductive capacity and tribological characteristics of poly (ethylene glycol-ran-propylene glycol) monobutyl ether as base oil of grease. *J. Tribol.* **138**(011801), 1–6 (2016)
41. Yu, S.R., Huang, Z.Q.: Dry sliding wear behavior of fly ash cenosphere/AZ91D Mg alloy composites. *J. Mater. Eng. Perform.* **23**, 3480–3488 (2014)
42. Lv, J.Z., Bai, M.L., Cui, W.Z., Li, X.J.: The molecular dynamic simulation on impact and friction characters of nanofluids with many nanoparticles system. *Nanoscale Res. Lett.* **6**, 200 (2011)
43. Kumar, K.R., Mohanasundaram, K.M., Arumaikkannu, G., Subramanian, R.: Effect of particle size on mechanical properties and tribological behaviour of aluminium/fly ash composites. *Sci. Eng. Compos. Mater.* **19**, 247–253 (2012)
44. Kumar, K.R., Mohanasundaram, K.M., Arumaikkannu, G., Subramanian, R., Anandavel, B.: Influence of particle size on dry sliding friction and wear behavior of fly ash particle-reinforced A380 Al matrix composites. *Eur. J. Sci. Res.* **60**, 428–438 (2011)
45. Chauhan, S.R., Kumar, A., Singh, I., Kumar, P.: Effect of fly ash content on friction and dry sliding wear behavior of glass fiber reinforced polymer composites—a Taguchi approach. *J. Miner. Mater. Charact. Eng.* **09**, 223–239 (2010)
46. Rapoport, L., Bilik, Y.: Hollow nanoparticles of WS₂ as potential solid-state lubricants. *Nature* **387**, 791–793 (1997)
47. Bucholz, E.W., Phillpot, S.R., Sinnott, S.B.: Molecular dynamics investigation of the lubrication mechanism of carbon nano-onions. *Comput. Mater. Sci.* **54**, 91–96 (2012)
48. Doig, M., Warrens, C.P., Camp, P.J.: Structure and friction of stearic acid and oleic acid films adsorbed on iron oxide surfaces in squalane. *Langmuir* **30**, 186–195 (2014)
49. Lundgren, S.M., Ruths, M., Danerlöv, K., Persson, K.: Effects of unsaturation on film structure and friction of fatty acids in a model base oil. *J. Colloid Interface Sci.* **326**, 530–536 (2008)